USCAP

www.nature.com/labinvest

ARTICLE

Bone morphogenetic protein induces bone invasion of melanoma by epithelial–mesenchymal transition via the Smad1/5 signaling pathway

Jing Gao[1], Ryusuke Muroya[1,2], Fei Huang[1], Kengo Nagata[3], Masashi Shin[4,5], Ryoko Nagano[3,6], Yudai Tajiri[3], Shinsuke Fujii[3], Takayoshi Yamaza[7], Kazuhiro Aoki[8], Yukihiko Tamura[9], Mayuko Inoue[10], Sakura Chishaki[10], Toshio Kukita[7], Koji Okabe[4], Miho Matsuda[1], Yoshihide Mori[2], Tamotsu Kiyoshima[3] and Eijiro Jimi[1,10]✉

Oral malignant melanoma, which frequently invades the hard palate or maxillary bone, is extremely rare and has a poor prognosis. Bone morphogenetic protein (BMP) is abundantly expressed in bone matrix and is highly expressed in malignant melanoma, inducing an aggressive phenotype. We examined the role of BMP signaling in the acquisition of an aggressive phenotype in melanoma cells in vitro and in vivo. In five cases, immunohistochemistry indicated the phosphorylation of Smad1/5 (p-Smad1/5) in the nuclei of melanoma cells. In the B16 mouse and A2058 human melanoma cell lines, BMP2, BMP4, or BMP7 induces morphological changes accompanied by the downregulation of E-cadherin, and the upregulation of N-cadherin and Snail, markers of epithelial–mesenchymal transition (EMT). BMP2 also stimulates cell invasion by increasing matrix metalloproteinase activity in B16 cells. These effects were canceled by the addition of LDN193189, a specific inhibitor of Smad1/5 signaling. In vivo, the injection of B16 cells expressing constitutively activated ALK3 enhanced zygoma destruction in comparison to empty B16 cells by increasing osteoclast numbers. These results suggest that the activation of BMP signaling induces EMT, thus driving the acquisition of an aggressive phenotype in malignant melanoma.

Laboratory Investigation (2021) 101:1475–1483; https://doi.org/10.1038/s41374-021-00661-y

INTRODUCTION

Malignant melanoma commonly occurs in the skin and typically develops from melanocytes, which produce melanin pigments. Malignant melanoma is a highly malignant tumor that causes lymphogenous and hematogenous metastasis[1,2].

Oral malignant melanoma is an extremely rare tumor, accounting for ~0.2–8% of all melanomas and ~0.5% of all oral malignancies[3,4]. Oral malignant melanoma appears to be more common in Asia (including Japan and India) and some African regions than in Western countries[5,6]. The prognosis of oral malignant melanoma is worse than that of cutaneous melanoma, with a 5-year survival rate of only 8–15%. Oral malignant melanoma most frequently occurs in the hard palate followed by the buccal mucosa, maxillary gingiva, and mandibular gingiva[7,8]. Due to the anatomic structure of the oral cavity, bone invasion and destruction are commonly seen in cases of melanoma of the hard palate and maxillary gingiva[9,10]. This bone invasion and destruction are associated with a poor prognosis. However, the molecular mechanism by which oral malignant melanoma acquires an aggressive phenotype is unclear[9,10].

Bone morphogenetic proteins (BMPs) are members of the transforming growth factor β (TGF-β) superfamily and are responsible for diverse cellular functions, including body patterning, organ morphogenesis, and the regulation of cell proliferation, differentiation, and apoptosis[11–14]. To date, more than 30 members of the BMP/TGF-β superfamily have been described in various species and a broad range of biological activities have been identified. BMP signaling is mediated by both type I and II receptors. BMP ligands bind three type I receptors, including type I receptor (ActRIA or ALK2), type IA (BMPR-IA or ALK3), and IB (BMPR-IB or ALK6) BMP receptors, and three type II receptors, including type II BMP receptor (BMPR-II), type IIA (ActR-IIA), and type IIB (ActR-IIB) activin receptors. Following ligand binding, type II receptors phosphorylate type I receptors. The activated type I

[1]Laboratory of Molecular and Cellular Biochemistry, Division of Oral Biological Sciences, Kyushu University, 3-1-1 Maidashi Higashi-ku, Fukuoka 812-8582, Japan. [2]Section of Oral and Maxillofacial Surgery, Division of Maxillofacial Diagnostic and Surgical Sciences, Faculty of Dental Science, Kyushu University, 3-1-1 Maidashi Higashi-ku, Fukuoka 812-8582, Japan. [3]Laboratory of Oral Pathology, Division of Maxillofacial Diagnostic and Surgical Sciences, Faculty of Dental Science, Kyushu University, 3-1-1 Maidashi Higashi-ku, Fukuoka 812-8582, Japan. [4]Department of Physiological Sciences and Molecular Biology, Fukuoka Dental College, 2-5-1 Tamura, Sawara-ku, Fukuoka 814-0175, Japan. [5]Oral Medicine Center, Fukuoka Dental College, 2-5-1 Tamura, Sawara-ku, Fukuoka 814-0175, Japan. [6]Department of Endodontology and Operative Dentistry, Division of Oral Rehabilitation, Faculty of Dental Science, Kyushu University, 3-1-1 Maidashi Higashi-ku, Fukuoka 812-8582, Japan. [7]Department of Molecular Cell Biology and Oral Anatomy, Division of Oral Biological Sciences, Faculty of Dental Science, Kyushu University, 3-1-1 Maidashi Higashi-ku, Fukuoka 812-8582, Japan. [8]Department of Functional Dentistry, Tokyo Medical and Dental University, 1-5-45 Yushima, Bunkyo-ku, Tokyo 113-8510, Japan. [9]Department of Bio-Matrix, Graduate School of Medical and Dental Sciences, Tokyo Medical and Dental University, 1-5-45 Yushima, Bunkyo-ku, Tokyo 113-8510, Japan. [10]Oral Health/Brain Health/Total Health Research Center, Faculty of Dental Science, Kyushu University, 3-1-1 Maidashi Higashi-ku, Fukuoka 812-8582, Japan. ✉email: ejimi@dent.kyushu-u.ac.jp

Received: 31 July 2020 Revised: 7 August 2021 Accepted: 7 August 2021
Published online: 9 September 2021

receptors can then phosphorylate receptor-specific Smads, such as R-Smad1/5, in the cytoplasm, thus enabling R-Smad1/5 to form a complex with Co-Smad4. This complex is then able to translocate into the nucleus where it regulates the expression of BMP-specific target genes[11–14].

Recent genetic studies of familial cancer syndromes strongly suggest that BMP signaling contributes to carcinogenesis[11]. Point mutations in Smad4 and BMPR-IA (ALK3) lead to familial juvenile polyposis[15]. Germ line mutations in ALK3 have been identified in a subset of families with Cowden syndrome, an inherited breast cancer syndrome[16]. Aberrations in BMP signaling have also been identified in various sporadic human cancers. Furthermore, several lines of evidence have shown that BMP signaling is deregulated in malignant melanoma. Previous studies have reported that several BMPs, especially BMP2, BMP4, and BMP7, are highly expressed in malignant melanoma cells in comparison to normal melanocytes[11,17]. These results strongly suggest that BMP plays an important role in the development or progression of malignant melanoma. However, the molecular mechanism by which BMP induces an aggressive phenotype in malignant melanoma is not clear.

Epithelial–mesenchymal transition (EMT) is a critical event in cancer progression and is characterized by morphological changes accompanied by a decreased expression of epithelial markers and an increased expression of mesenchymal markers[18–20]. TGF-β is a well-known, widely studied prototypical stimulator of EMT[18,19]. Furthermore, BMP is a protein found in the bone matrix [11–14] and therefore might be involved in bone invasion by malignant melanoma. In this study, we investigated whether or not BMP induces EMT, invasive activity, and bone metastasis of malignant melanoma.

MATERIALS AND METHODS

Reagents

Purified recombinant human BMP2 and TGF-β1 were purchased from R&D Systems (Minneapolis, MN, USA). Purified recombinant human BMP4, BMP7 and Activin A1 were obtained from Peprotech (Cranbury, NJ, USA) and Miltenyui Biotec (Bergisch Gladbach, Germany), respectively. For western blotting, anti-phosphorylated Smad1/5 (#11971), anti-Smad1 (#9743), anti-Smad4 (no. 46535), anti-Snail (#3895), anti-phosphorylated extracellular related kinase (ERK)1/2 (#9101S), anti-ERK1/2 (#9102), anti-phosphorylated Smad3 (#9520), and anti-Smad2/3 (#8685) antibodies were obtained from Cell Signaling Technology, Inc. (Beverly, MA, USA). Anti-mouse E-cadherin (#610181) and N-cadherin (#610920) antibodies were purchased from BD Bioscience (Franklin Lakes, NJ, USA). LDN193189 and anti-β-actin (#AC-15) antibody were purchased from Sigma-Aldrich (St. Louis, MO, USA). SB431542 was purchased from Fuji Film Wako Pure Chemical Corp. (Osaka, Japan). Anti-V_5 antibody (#M215-3) was obtained from Medical and Biological Laboratories (Nagoya, Japan). For immunohistochemistry, anti-phosphorylated Smad1/5 (#700047) monoclonal antibody (31H14L11) were obtained from Thermo Fisher Scientific (Waltham, MA, USA).

Malignant melanoma patient tissue samples and histology

The experimental procedures conducted in this study were reviewed and approved by the Kyushu University Research Ethics Committee (approval numbers 27–362 and 30–235) and informed written consent was obtained from the patients. Malignant melanoma tumor samples from five patients and benign oral nevus samples from five patients were diagnosed at the Pathology Department, Kyushu University Hospital, Japan, and these samples were examined in this study. The tissues were fixed with 4% paraformaldehyde buffered by phosphate buffered saline (PBS) and embedded in paraffin. Five-micrometer thick paraffin sections were stained with H&E or processed for immunohistochemical staining with anti-phosphorylated Smad1/5 monoclonal antibody (Thermo Fisher Scientific, 1:400) using the polymer detection system (Histofine Simple Stain MAX PO, Nichirei, Tokyo, Japan). Endogenous peroxidase activity was inhibited by treatment with 3% H_2O_2 in methanol. Non-specific protein binding was blocked with 10% normal goat serum (Nichirei). The immunoreactivity was visualized with a solution of 3,3′-diaminobenzidine and <0.1% hydrogen peroxide (DAB substrate solution, Nichirei). Subsequently, the immunohistochemical stained sections were counterstained with hematoxylin. Antibody dilute solution (1% bovine serum albumin, 0.2% Triton X-100 and 0.02% sodium azide in PBS) was used as a negative immunohistochemical control. All samples were observed under a microscope equipped with a Microscope Digital Camera System DP-72 (Olympus, Tokyo, Japan).

Analysis of the TCGA cancer dataset

The BMP, BMP receptor, and Smad1/5 gene expression data for 103 primary skin melanomas and 368 metastatic melanomas were obtained from The Cancer Genome Atlas (TCGA) (http://tcga-data.nci.nih.gov/tcgaHome2.jsp).

Cell culture

B16 mouse and A2058 human melanoma cells were obtained from RIKEN BioResource Center and Japanese Collection of Research Bioresources (JCRB) Cell Bank (Tokyo, Japan) in January 2016 and were authenticated by JCRB using short tandem repeat polymerase chain reaction, which was performed with a PowerPlex® 16 STR System (Promega, Madison, WI, USA). Cells were cultured in Dulbecco's modified Eagle's medium (DMEM) containing 5% fetal bovine serum (FBS), 100 units/ml penicillin, and 100 µg/ml streptomycin (Sigma-Aldrich) in a humidified atmosphere of 5% CO_2 at 37 °C.

Western blotting

For immunoblotting, whole-cell lysates were resolved on sodium dodecyl sulfate (SDS)-polyacrylamide gels and transferred to PVDF membranes. Membranes were then incubated overnight at 4 °C with antibodies diluted to 1:1000 in a 5% dry milk or bovine serum albumin solution containing 0.01% azide in TTBS (10 mM Tris-HCl, 50 mM NaCl and 0.25% Tween-20). Finally, membranes were incubated with a horseradish peroxidase-conjugated secondary antibody and immunoreactive proteins were visualized using an Enhanced ChemiLuminescence kit (Merck Millipore, Burlington, MA, USA).

Luciferase assays

Luciferase assays were performed as previously described[21]. B16 cells were transfected with the Id-WT4F-luciferase reporter, which was kindly provided by Dr. Katagiri (Saitama Medical University, Saitama, Japan), using Lipofectamine 3000 (Invitrogen, Carlsbad, CA, USA) according to the manufacturer's instructions. The luciferase activity was measured using a dual luciferase reporter assay system (Promega, Madison, WI, USA).

Cell invasion assays

Cell migration was assessed in a modified Boyden chamber containing a Matrigel-coated porous membrane. B16 cells were seeded in the upper chamber. LDN193189 (0 or 200 nM) was placed in the upper chamber 2 h prior to BMP2 treatment, and BMP2 was added to the lower chamber at 100 ng/ml. The chamber was then incubated for an additional 24 h. Next, the cells attached to the upper surface of the membrane were scraped off, and the cells that had migrated to the lower surface were fixed and stained with DAPI.

Zymography

Serum-free conditioned medium was collected from confluent B16 cells incubated in the presence of reagents for 24 h. The conditioned medium was resolved via 10% SDS-polyacrylamide gel electrophoresis in the presence of 1 mg/ml gelatin. The resulting gel was washed in 10 mM Tris (pH 8.0) containing 2.5% Triton X-100 and then incubated for 16 h in reaction buffer (50 mM Tris, pH 8.0, 0.5 mM $CaCl_2$, and 10^{-6} M $ZnCl_2$) at 37 °C. After staining with Coomassie brilliant blue, the gelatinases appeared as clear bands of lysed gelatin against a blue background.

Cell proliferation assays

B16 cell proliferation was measured using a Cell Counting Kit-8 (Dojindo, Kumamoto, Japan) according to the manufacturer's instructions.

Generation of a stable B16 cell line expressing a constitutively active form of BMPR1A

The V5-tagged constitutively active form of type I BMP receptor, which substituted aspartic acid for the glutamine residues at 233 and 203 (BMPRIA:V5-CaALK3/pDEF)[22] was kindly provided by Dr. Katagiri (Saitama Medical University). B16 cells were seeded in 35-mm plates, cultured for 24 h, and then transfected with 1 µg of the V5-ALK3Ca expression vector using 3 µL of Lipofectamine 3000. The pcDEF empty vector was transfected into B16 cells as a negative control. Transfection was performed according

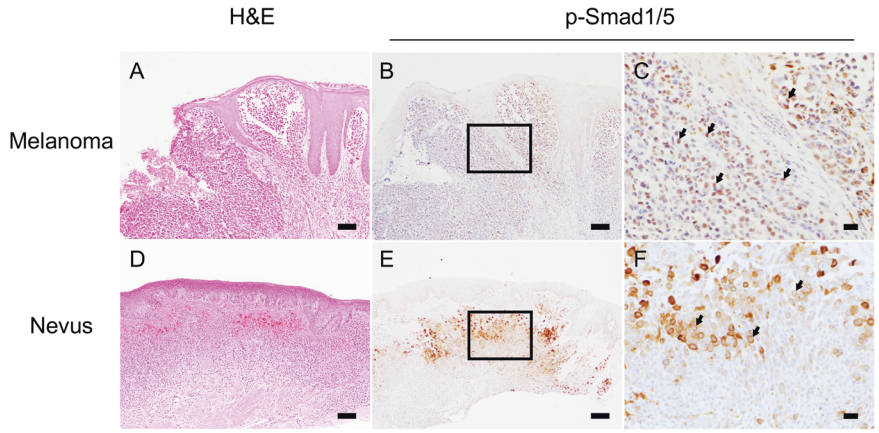

Fig. 1 The comparison of the expression pattern of phosphorylated-Smad1/5 in malignant melanoma and benign oral nevus patient samples. Five malignant melanomas and five benign oral nevus patient samples were stained with H&E (**A**, **D**), and with anti-p-Smad1/5 and then stained with hematoxylin to detect nuclei (**B**, **C**, **E**, **F**). One amelanotic malignant melanoma and benign oral nevus section representative of five samples is shown. Phosphorylated Smad1/5 was observed in the nucleus of the malignant melanoma cells and in the cytoplasm of the benign oral nevus samples. Bar = 300 μm (**A**, **B**, **D**, **E**), Bar = 50 μm (**C**, **F**).

to the manufacturer's instructions. At 48 h post-transfection, the medium was switched to complete culture medium containing 800 μg/ml G418. After 2 weeks of incubation in this medium, G418-resistant colonies were selected. Cells were maintained in G418 for 6–10 days and expanded.

Animal model of bone invasion

Sixteen male B6 mice (age, 8–10 weeks; body weight, 20 g) obtained from CLEA (Tokyo, Japan) were used to modify an established model of mandible invasion by oral squamous cells[23,24]. The mice were randomly separated into two groups with similar average body weights and anesthetized by isoflurane inhalation. Then, 0.1 ml of either empty vector-transfected (empty) B16 cells or V5-CaALK3/pDEF-transfected B16 cells (1.0×10^5/ml) resuspended in DMEM was injected into the left masseter region. The tumor size was assessed using calipers, and the tumor volume was calculated using the following formula: width$^2 \times$ length $\times$ 0.52[25]. At the end of week 3, all surviving mice were euthanized, and the heads of the mice were fixed in 3.7% formaldehyde (Wako Pure Chemical Industries, Ltd., Osaka, Japan).

Three-dimensional reconstructed images of the heads were obtained via microfocal computed tomography (μ-CT; ScanXmate-E090; Comscan, Kanagawa, Japan) as previously described[23,24]. The reconstructed μ-CT images were used to score the extent of zygoma destruction as follows: 0, normal; 1, asymmetric; 2, displaying a hairline fracture; 3, zygoma completely separated; and 4, destruction of more than 1/3 of the zygoma. The images were evaluated in a blinded manner by eight researchers[23–25].

Formaldehyde-fixed paraffin-embedded sections (thickness, 5 μm) were obtained from the region posterior to the lower third molar and stained with hematoxylin & eosin (H&E) and tartrate-resistant acid phosphatase (TRAP). For each specimen, five tumor fields were randomly selected, and the number of TRAP-positive multinucleated cells (TRAP$^+$ MNCs) was quantified. The data are expressed as the number of TRAP$^+$ MNCs/bone surface (mm^2)/section.

Data analysis

Comparisons were performed using an unpaired Student's *t* test. These data are expressed as the mean ± standard deviation (SD), and *p* values of <0.05 were considered to indicate statistical significance. For the in vivo experiments, comparisons were performed via a factorial analysis of variance. When significant *F* values were detected, Fisher's PLSD post hoc test was performed for between-group comparisons. The data are expressed as the mean ± SD, and *p* values of <0.05 were considered to indicate statistical significance.

RESULTS

The expression of p-Smad1/5 in malignant melanoma patient samples

Previous reports showed that malignant melanoma cells expressed several BMPs, including BMP 2, 4, 5, 7, and its receptor, BMP-IA[11,17,26], suggesting that BMPs produced by malignant melanoma cells act on themselves and induce aggressiveness. Thus, to confirm that the BMP signal is activated in malignant melanoma, we first examined the expression of phosphorylated Smad1/5 as an indicator of BMP signal activation in human malignant melanoma samples compared with the benign oral nevi by immunostaining using phosphorylated Smad1/5 antibody. Figure 1A and D showed a representative H&E image of a malignant melanoma patient sample and nevus, respectively. Phosphorylated Smad1/5 was observed in malignant melanoma cells, but not normal epithelial cells (Fig. 1B and Supplementary Fig. 1C, F). P-Smad1/5 was strongly stained in the nuclei of malignant melanoma cells (Fig. 1C and Supplementary Fig. 1F). P-Smad1/5 was observed in the cytoplasm, but not in the nuclei of the benign oral nevi (Fig. 1E, F). Stained without primary antibody and then counterstained with hematoxylin to detect nuclei (Supplementary Fig. 1B, E). Some nuclei, which were considered to be vascular endothelial cells, were not positive for p-Smad1/5 (Supplementary Fig. 1F). These results prompted us to investigate the role of BMP signaling in the alteration of the characteristics of malignant melanoma cells.

To further analyze whether the BMP expression and/or activation of this pathway is closely associated with the disease stages, aggressiveness, prognosis and/or clinical outcomes of melanoma, we investigated the changes in the BMP, BMP receptor and Smad1/5 gene expression, using The Cancer Genome Atlas (TCGA) dataset. Unfortunately, there were no data for oral melanoma; thus, we analyzed the skin melanoma data. Moreover, since there was only one case of normal benign nevus, the expression of these genes was compared between the primary tumors ($n = 103$) and metastatic tumors ($n = 368$). The BMP2, 4, and 7 expression of the primary and metastatic lesions did not differ to a statistically significant extent (Supplementary Fig. 2A), but the expression of BMPRIA (ALK3) was high in the metastatic lesions, and conversely, the expression of BMPRIB (ALK6) was decreased in the metastatic lesions (Supplementary Fig. 2B). The expression of BMPRII in the primary and metastatic lesions did not differ to a statistically significant extent (Supplementary Fig. 2B). Furthermore, the expression of Smad5, but not Smad1, was higher in the metastatic lesions in comparison to the primary tumors (Supplementary Fig. 2C). These results indicate that the BMPIA (ALK3)-mediated activation of BMP signals is correlated with the aggressiveness of melanoma.

BMP signaling is activated in melanoma cells

Previous studies have shown that the enhancement of BMP signaling by the overexpression of BMP2, BMP4, or BMP7, and

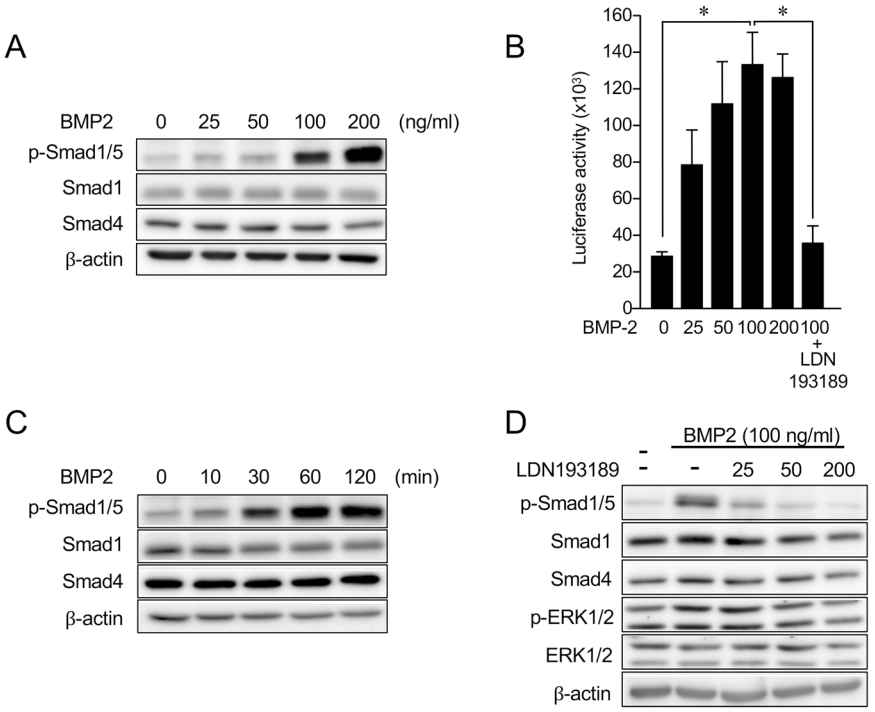

Fig. 2 BMP signaling is activated in B16 melanoma cells. A B16 cells were treated with various concentrations of BMP2 for 30 min. Phosphorylated Smad1/5, Smad1, and Smad4 were examined by Western blotting. β-actin was used as a loading control. Similar results were obtained from three independent experiments. **B** B16 cells were transiently transfected with an Id-WT4F-luciferase reporter and then treated with or without various concentrations of BMP2 in the presence or absence of LDN193189 (200 nM) for 24 h. The luciferase activity of the cells was assessed after 24 h. The data are expressed as the mean ± SD ($n = 3$). *$p < 0.01$. Similar results were obtained from 3 independent experiments. **C** B16 cells were treated with BMP2 (100 ng/ml) for the indicated lengths of time. Phosphorylated Smad1/5, Smad1, and Smad4 were examined by Western blotting. β-actin was used as a loading control. Similar results were obtained from three independent experiments. **D** B16 cells were pretreated with various concentrations of LDN193189 for 2 h and then treated with BMP2 (100 ng/ml) for 30 min. Phosphorylated Smad1/5, Smad1, Smad4, phosphorylated ERK, and ERK were examined by Western blotting. β-actin was used as a loading control. Similar results were obtained from three independent experiments.

mutations of BMP receptors are involved in the progression of cancer cells, including melanoma, by enhanced cell migration and invasion[11,17,26–33]. Since BMP2 has been reported to be involved in the development and progression of many cancers[33–37], we next examined whether BMP2 induces Smad1/5 phosphorylation in melanoma cells. BMP2 induced Smad1/5 phosphorylation in a dose-dependent manner in both B16 mouse and A2058 human melanoma cells (Figs. 2A and 4A). Furthermore, either BMP4 or BMP7 also induced Smad1/5 phosphorylation (Supplementary Fig. 3A). BMP2 (100 ng/ml) induced maximal levels of Id-1 transcriptional activity (Fig. 2B); thus, we decided to use BMP2 at 100 ng/ml in subsequent experiments. Smad1/5 phosphorylation was detected within 30 min and reached peak levels between 60 and 120 min (Fig. 2C). Pretreatment with LDN193189, a highly potent small-molecular BMP inhibitor that inhibits BMP type I receptors (ALK2, ALK3, and ALK6) suppressed the BMP2-induced phosphorylation of Smad1/5 in a dose-dependent manner, while ERK activation remained unchanged (Fig. 2D). LDN193189 (200 nM) also inhibited BMP2-induced Id1 transcriptional activity (Fig. 2B).

BMPs induce EMT in melanoma cells

Both B16 and A2058 cells were treated with BMP2 (100 ng/ml) for 0 to 48 h. Treated cells began to acquire an elongated and spindle-like morphology 24 h after BMP2 treatment, while the cells in the control group showed no morphological changes (Figs. 3A and 4B). BMP2 slightly suppressed the proliferation of B16 melanoma cells (Supplementary Fig. 4). BMP2 treatment resulted in the downregulation of E-cadherin, and the upregulation of N-cadherin and Snail, both of which are well-characterized markers of EMT (Figs. 3B and 4C). Either BMP4 or BMP7 also induced an elongated and spindle-like morphology with the downregulation of E-cadherin, and the upregulation of N-cadherin and Snail in B16 cells (Fig. S3B,C). Pretreatment with LDN193189 suppressed BMP2-induced morphological changes, E-cadherin downregulation, and N-cadherin and Snail upregulation in B16 cells and A2058 cells (Figs. 3C, D and 4B, C), suggesting that BMP/Smad signaling induces EMT in melanoma cells.

BMP2 promotes B16 melanoma cell migration and invasion

EMT is an important process that is required during tumor progression to promote invasive and metastatic properties[18–20]. BMP2 markedly enhanced the invasion of B16 cells (Fig. 5A,B), while pretreatment with LDN193189 significantly inhibited BMP2-induced cell invasion. The viability of cells treated with LDN193189 for up to 24 h was comparable to that of BMP2-treated cells (Supplementary Fig. 4). We further examined the effect of BMP2 on the production of two major gelatinases, MMP-2 and MMP-9. The production of MMP-2 and MMP-9 was noticeably increased following BMP2 treatment (Fig. 5C), while pretreatment with LDN193189 suppressed this production (Fig. 5C). Taken together, these findings suggest that BMP2 can promote B16 cell invasion during EMT in vitro.

Generation of B16 melanoma cells expressing constitutively activated BMP receptor

Since ALK3 is a common type I BMP receptor of BMP2, BMP4, and BMP7, but not TGFβ and Activin A[13,14]. The constitutively activated ALK3 enhances BMP signaling[22,38,39]. To investigate the role of BMP signaling in melanoma progression in vivo, we generated a stable B16 cell line expressing constitutively activated ALK3 (V5-CaALK3). Smad1/

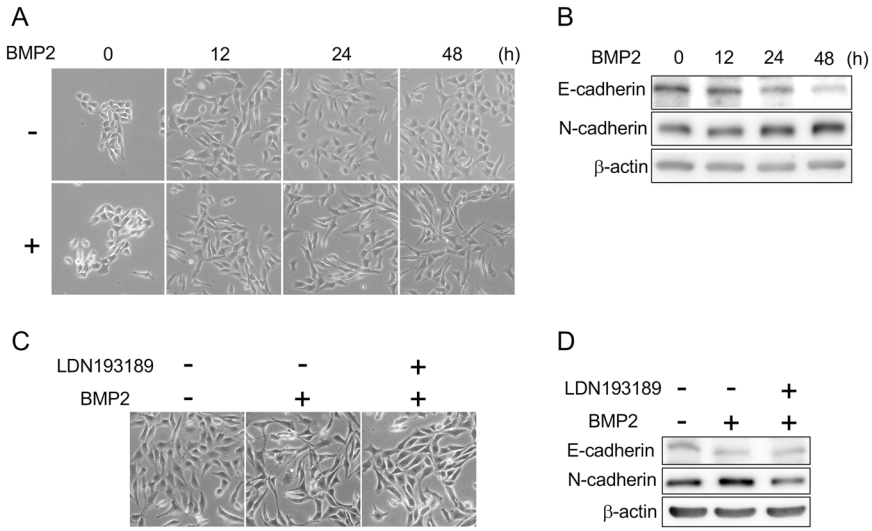

Fig. 3 BMP2 induces epithelial–mesenchymal transition (EMT) in B16 melanoma cells. A B16 cells were treated with or without BMP (100 ng/ml) for the indicated lengths of time. Morphological changes were observed by phase contrast microscopy. **B** Western blotting was used to examine the expression of E-cadherin, N-cadherin, and Snail in B16 cells treated with BMP (100 ng/ml) for the indicated lengths of time. β-actin was used as a loading control. Similar results were obtained from three independent experiments. **C** B16 cells were pretreated with LDN193189 (200 nM) for 2 h and then with BMP2 (100 ng/ml) for 48 h. Morphological changes were observed by phase contrast microscopy. **D** Western blotting was used to examine the expression of E-cadherin, N-cadherin, and Snail in B16 cells pretreated with LDN193189 (200 nM) for 2 h and BMP2 (100 ng/ml) for an additional 48 h.

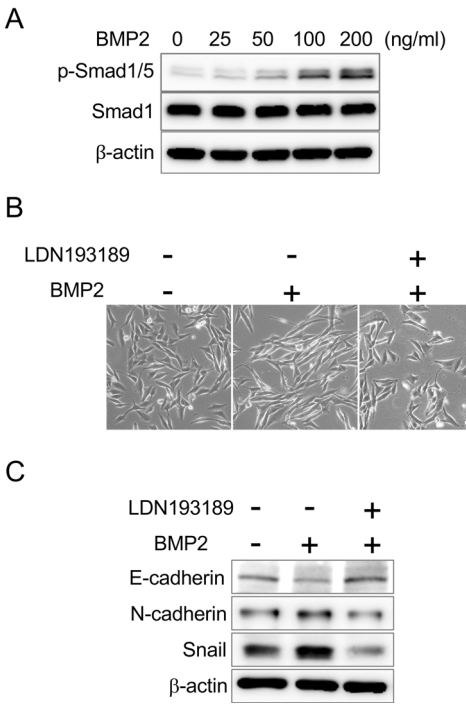

Fig. 4 BMP2 induces epithelial–mesenchymal transition (EMT) in A2058 human melanoma cells. A A2058 cells were treated with various concentrations of BMP2 for 30 min. Phosphorylated Smad1/5, and Smad1 were examined by Western blotting. β-actin was used as a loading control. Similar results were obtained from three independent experiments. **B** A2058 cells were pretreated with LDN193189 (200 nM) for 2 h and then with BMP2 (100 ng/ml) for 48 h. Morphological changes were observed by phase contrast microscopy. **C** Western blotting was used to examine the expression of E-cadherin, N-cadherin, and Snail in A2058 cells pretreated with LDN193189 (200 nM) for 2 h and BMP2 (100 ng/ml) for an additional 48 h.

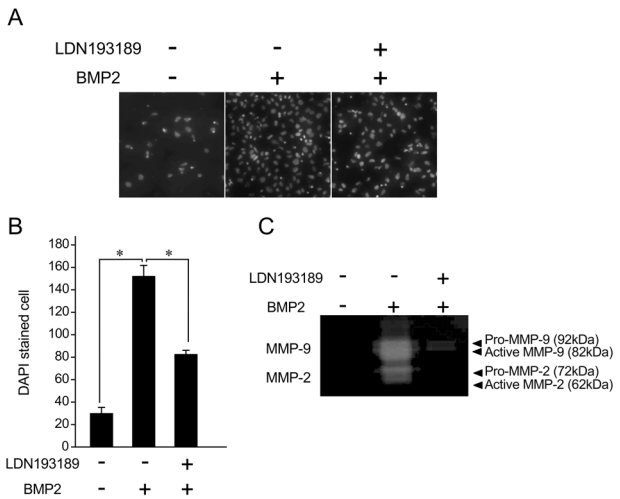

Fig. 5 BMP2 promotes B16 melanoma cell migration and invasion. A, **B** B16 cells were suspended in serum-free DMEM and seeded in the upper chamber above a Matrigel-coated porous membrane. LDN193189 (0 or 200 nM) was placed in the upper chamber 2 h before BMP2 treatment. Next, BMP2 (100 ng/ml) was added to the lower chamber and cells were incubated for 14 h. The cells attached to the upper surface of the membrane were then scraped off, those that had migrated to the lower surface were fixed and stained with DAPI and quantified. The data are expressed as the mean ± SD ($n = 3$). *$p < 0.01$. Similar results were obtained from 3 independent experiments. **C** Cells were incubated in serum-free DMEM for 24 h in the presence or absence of BMP2 (100 ng/ml) and pretreated with or without LDN193189 (200 nM). The conditioned media was analyzed by gelatin zymography. Similar results were obtained from three independent experiments.

5 phosphorylation was observed in V5-CaALK3 B16 cells but not in empty vector (Empty) transfected B16 cells without BMP2 (Fig. 6A). V5-CaALK3 B16 cells were spindle-shaped and showed E-cadherin

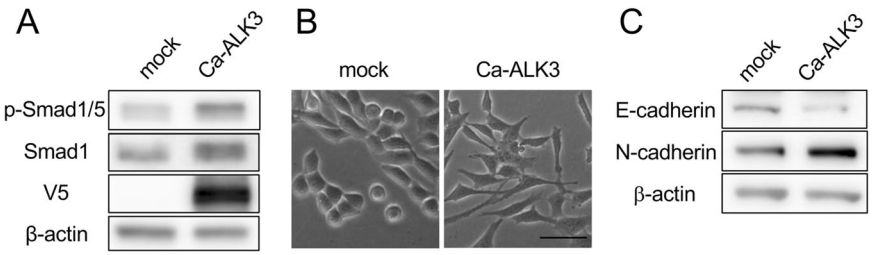

Fig. 6 Generation of B16 cells expressing constitutively activated BMP receptor. A B16 cells were seeded in 35-mm plates, cultured for 24 h, and transfected with 1 μg of V5-ALK3Ca expression vector (V5-CaALK3 B16 cells). As a negative control, the pcDEF empty vector was introduced into B16 cells (empty B16 cells). Phosphorylated Smad1/5 and Smad1 were examined by Western blotting. β-actin was used as a loading control. Similar results were obtained from three independent experiments. **B** V5-CaALK3 B16 or empty B16 cells were cultured for 48 h. Morphological changes were observed by phase contrast microscopy. **C** Western blotting was used to examine the expression of E-cadherin and N-cadherin V5-CaALK3 B16 or empty B16 cells.

downregulation and N-cadherin upregulation (Fig. 6B, C), suggesting that V5-CaALK3 induces EMT in B16 cells.

Next, it was confirmed that the established cell line mainly transduces BMP signals. As described above, when B16 cells were stimulated with BMP2, the cells became spindle-shaped and scattered, but when stimulated with TGF-β1, they became a spindle-shaped mass. The morphology of V5-Ca-ALK3 B16 cells closely resembled that of BMP2-treated cells (Supplementary Fig. 5A). The V5-Ca-ALK3 B16 cells had significantly higher Id-1 transcriptional activity in comparison to empty B16 cells, and BMP2 stimulation further increased the transcriptional activity, whereas TGF-β1 or Activin A1 failed to enhance the basal transcriptional activity of V5-Ca-ALK3 B16 cells (Supplementary Fig. 5B). In addition, neither TGF-β1 nor Activin A1 enhanced the Smad3 phosphorylation in V5-Ca-ALK3 B 16 cells in comparison to empty B16 cells (Supplementary Fig. 5C). Finally, when V5-Ca-ALK3 B16 cells were treated with LDN193189, they changed from a spindle shape to a cuboidal shape, and the decreased E-cadherin expression was slightly recovered and the N-cadherin expression was decreased. Whereas SB431542, an inhibitor of TGF-β signaling, did not affect the morphology of V5-Ca-ALK3 B16 cells or the changes of the E-cadherin or N-cadherin expression (Supplementary Fig. 5D, E). These results suggest that V5-Ca-ALK3 B16 cells were mainly activated in BMP signals.

Constitutively activated BMP signaling enhances bone invasion by B16 melanoma cells

To investigate the role of BMP signaling in B16 cells in vivo, we injected either V5-CaALK3 B16 cells or empty B16 cells into the left masseter region and allowed tumor cells to grow over 4 weeks. The body weights of the V5-CaALK3 B16 cell group and the empty B16 cell group were comparable (Fig. 7A). The tumors of the V5-CaALK3 B16 cell group were larger than those of the empty B16 cell group (Fig. 7B). Micro-CT images revealed the typical extent of bone invasion in each group, and the zygomatic bone destruction score is shown in Fig. 7C. In the empty B16 cell group, although the fracture line could be observed, zygoma continuity was maintained. In contrast, in the V5-CaALK3 B16 cell group, the zygoma was thin or destroyed (Fig. 7C, D).

A histological analysis revealed that, in the empty B16 cell group, cells typically lined the zygoma and an irregular bone surface filled with osteoclasts could be observed (Fig. 7E). In contrast, in the V5-CaALK3 B16 cell group, cells successfully infiltrated into the zygoma and numerous bigger osteoclasts could easily be identified (Fig. 7E, F). These results indicate that constitutively activated BMP signaling induces an aggressive phenotype in malignant melanoma and leads to bone invasion in vivo.

DISCUSSION

BMPs play an important role in the development and progression of malignant melanoma as well as other carcinomas[11,18,27–29]. Previous reports have shown that BMP2, BMP-6, BMP-7, and BMP-8 were upregulated in malignant melanoma cell lines in comparison to normal melanocytes and that this increased expression was involved in the development of malignant melanoma[11,26]. For example, the expression of BMP7 is correlated with aggressiveness in melanoma[11,27]. Single-nucleotide polymorphisms in the BMP4 gene can affect the expression of BMP4 mRNA, which is correlated with the aggressiveness of cutaneous malignant melanoma[30]. BMP2 induces melanin synthesis by increasing the expression of the tyrosinase gene[31]. Furthermore, all six BMP receptors are also expressed to varying degrees in melanoma cell lines[11]. In this study, we showed that p-Smad1/5 was observed in the nucleus in amelanotic malignant melanoma cells, but not in normal epithelial cells or benign oral nevi, indicating that BMP signaling is constitutively activated in melanoma cells. The TCGA dataset analysis also showed the increased expression of BMPIA receptors and Smad5 in metastatic lesions in comparison to the primary melanoma tumors, suggesting that BMP signal activation is correlated with malignancy in melanoma. This prompted us to investigate the biological role of BMP in melanoma aggressiveness both in vitro and in vivo.

Previous studies have shown that BMPs are extensively involved in the regulation of cellular functions in malignant melanoma cells, ranging from cell growth and death to cell migration, invasion, and EMT[11,18,27–29]. BMP regulates cell growth, although reports regarding whether BMP-mediates the inhibition or promotion of tumor growth are contradictory[32]. Melanoma cells express high levels of BMP7 and are able to escape BMP-induced growth inhibition[11,27]. One possible mechanism by which melanoma cells are capable of bypassing BMP7-induced growth inhibition is through the inhibition of BMP signaling via the upregulation of the BMP antagonist, Noggin[27]. The inhibitory action of BMP2 on tumor cells is associated with the Smad1- and Smad4-dependent upregulation of the cyclin-dependent kinase inhibitors p21 and p27[33–35]. In contrast, BMP2 enhances pancreatic carcinoma cell proliferation in vitro and in non-small cell lung carcinoma in vivo[36,37]. In this study, BMP2 slightly suppressed the proliferation of B16 melanoma cells in vitro, although the tumor volume in the V5-CaALK3 B16 cell group tended to larger than that in the empty B16 group in vivo. These results suggest that the effects of BMPs on melanoma cell growth depend on the cell type, differentiation stage, and the in vitro or in vivo context.

BMP induces apoptosis in many nontumor and tumor cells by inducing cell cycle arrest in the G1 phase, downregulating Bcl-xL, and activating the DNA damage response[40,41]. Recently, a cDNA microarray analysis identified death inducer-obliterator 1 (Dido1) as a BMP-specific Smad-regulated target gene in melanoma. This microarray analysis compared groups treated with BMP and with Dorsomorphin, a Smad-specific inhibitor that works to block kinase activity in the BMPR1-treated group[28]. The expression of Dido1 in

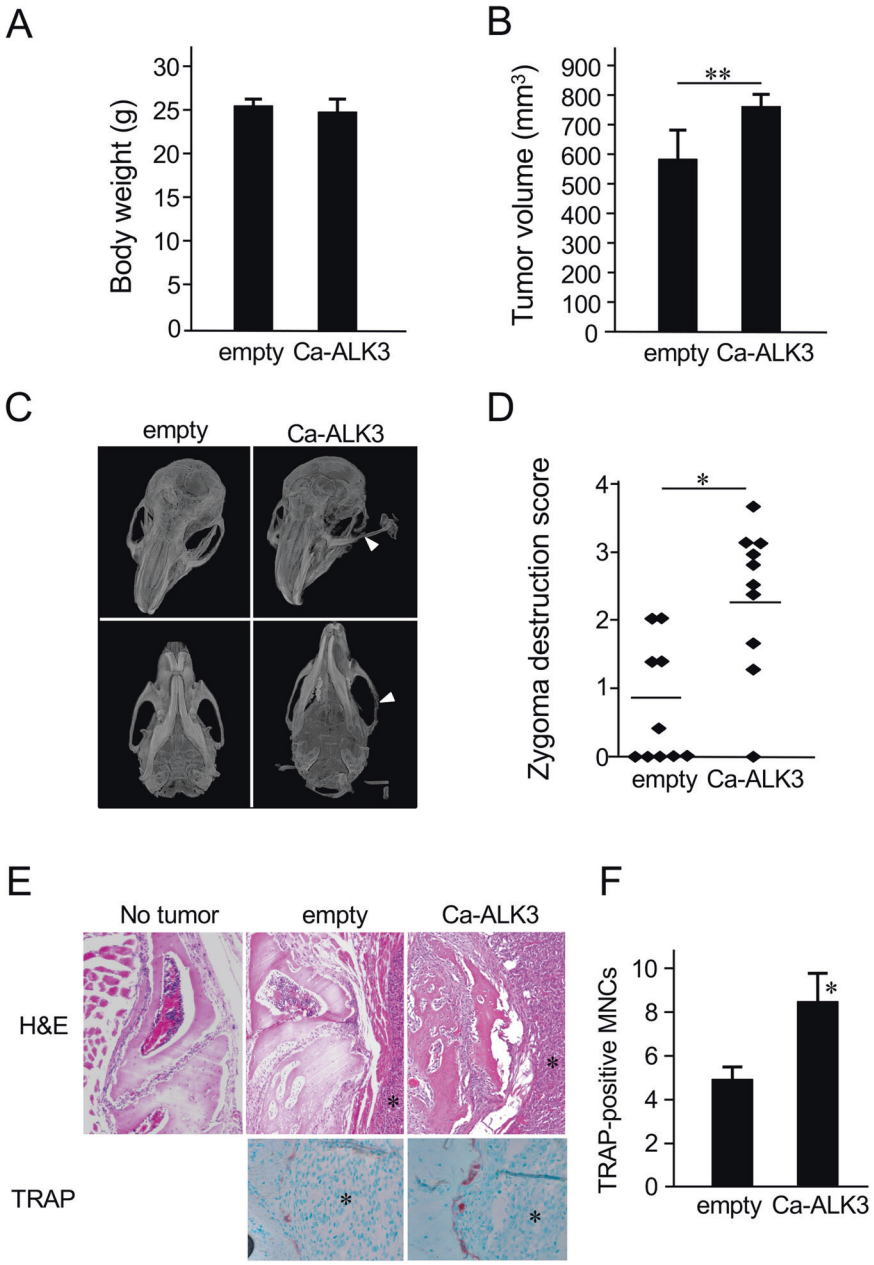

Fig. 7 Constitutively activated BMP signaling enhances bone invasion by B16 melanoma cells. A V5-CaALK3 B16 or empty B16 cells were injected into the left masseter of 8-week-old B6 mice. Body weights were measured 28 weeks after tumor cell inoculation. The data are expressed as the mean ± SD ($n = 10$). **B** The tumor volume was assessed using calipers and calculated using the following formula: width^2 × length × 0.52. The data are expressed as the mean ± SD ($n = 10$). **$p < 0.05$. **C** Reconstructed μ-CT images of zygoma destruction in the V5-CaALK3 B16 and empty B16 cell groups. Arrowheads indicate a fracture line in the zygoma. Bar = 8 mm. **D** The severity of zygoma destruction was assessed based on clinical scoring of the V5-CaALK3 B16 ($n = 10$) or empty B16 cells group ($n = 10$). *$p < 0.01$. **E** Twenty-eight days after B16 cell inoculation, tissues were fixed in 3.7% formaldehyde, decalcified in 5% formic acid, sectioned on the coronal axis and stained with H&E and TRAP. Bar = 200 μm; magnification 40× (upper panels), 200× (lower panels). *: tumor. **F** In each specimen, five tumor fields were randomly selected, and the number of TRAP$^+$ MNCs was counted. The data are expressed as the mean ± SD of the number of TRAP$^+$ MNCs/bone surface (mm^2)/section ($n = 5$). *$p < 0.01$.

melanoma cell lines and tissues is higher than that in normal melanocytes. siRNA-mediated knockdown of Dido1 induced apoptosis and suppressed melanoma cell migration and invasion. Growth differentiation factor 6 repressed the expression of the proapoptotic factor SOX9 by activating BMP signaling, thus inhibiting cell death[42]. Although we did not observe any marked differences in cell death according to the presence of BMP2 in vitro, one possible mechanism of action might be that BMP enhances migration and invasion by preventing melanoma cell apoptosis.

BMP enhances EMT in both cancer cells and normal epithelial cells during the restoration of disrupted epithelium[43,44]. These previous results prompted us to examine whether or not BMPs induces EMT in melanoma cells. BMP2, BMP4 or BMP7 induced a time-dependent morphological transformation of B16 or A2058 melanoma cells from a round shape to a spindle shape accompanied by the downregulation of E-cadherin and the upregulation of N-cadherin and Snail. Pretreatment with LDN193189 negated these effects. Furthermore, Ca-ALK3 B16 cells led to morphological changes similar to BMP2-treated B16

cells and LDN193189, but not SB431542 suppressed the morphological changes by inhibiting EMT, suggesting that the activation of BMP signaling induces EMT in B16 cells. Consistent with these results, Nodal, a member of the TGF-β superfamily, promoted B16 cell aggressiveness by inducing EMT[45]. These results indicate that TGF-β superfamily members induce EMT in melanoma cells, driving the acquisition of an aggressive phenotype.

The proteolysis and degradation of extracellular matrix structures are essential for melanoma cell dissemination[11]. MMPs, including MMP-1, MMP-2, MMP-3, MMP-9, and MMP-13, play a role in melanoma invasion via the degradation of the extracellular matrix[46,47]. A previous report showed that melanoma cell clones with reduced BMP activity, which was induced by stable transfection with antisense BMP4 or with the BMP inhibitor chordin, had reduced expression levels of MMP-1, MMP-2, MMP-3, and MMP-9[48]. BMPs may regulate the expression of MMPs in a direct or indirect manner. In addition to the Smad signaling pathway, BMPs activate the MAPK pathway, including ERK, c-Jun N-terminal kinase, and p38. Downstream transcription factors, including Fos/Jun family members, then induce the expression of MMP via an AP-1 binding site[49]. In this study, constitutively phosphorylated ERK was observed in B16 cells in the presence or absence of BMP2, and pretreatment with LDN193189 suppressed the BMP2-induced activity of MMP-2 and MMP-9 without affecting the activation of ERK. Further studies are needed to determine whether the Smad or other MAPK pathways are involved in the expression of MMP that is induced by BMP2.

We previously established a mouse model of bone invasion by oral squamous cell carcinoma[23,24]. In this study, we modified this model using B16 cells. Although we first tried to inject B16 cells into the hard palate, the cells failed to engraft. We therefore injected B16 cells into the left masseter region and then assessed the degree of zygoma destruction as a proxy for bone invasion. The injection of parental B16 cells did not destroy the zygoma, possibly due to a weakly aggressive phenotype. Since ALK3 is a common type I BMP receptor of BMP2, BMP4, and BMP7, but not TGFβ and Activin A, and mutations in ALK3 have been reported to be involved in the development of hereditary breast cancer[14,16], we also generated a stable B16 cell line expressing CaALK3 and injected these cells into the left masseter region. Tumors were larger in the V5-CaALK3 B16 cell group and zygoma destruction was much more apparent than that in the empty B16 cell group, suggesting that the activation of BMP signaling leads to acquired aggressiveness in B16 cells. A few lung metastases were observed in the V5-CaALK3 B16 cell group; however, due to the very small number, a more detailed investigation is required in the future. The role of the BMP-EMT axis in melanoma has been previously reported[11,50,51]; however, verification of the observation in a convincing in vivo mouse model is lacking. Thus, our study is novel and different from other studies.

In conclusion, BMPs play several biological roles, including being involved in the regulation of cell growth, apoptosis, EMT, and angiogenesis, in order to induce an aggressive phenotype in melanoma. In the present study, we showed that BMP2, BMP4, or BMP7 induces EMT and extracellular matrix degradation in B16 and A2058 melanoma cells via a Smad-dependent mechanism. The constitutive activation of BMP signaling via stable transfection with a constitutively activated form of ALK3 induced an aggressive phenotype and allowed B16 cells to invade bone in vivo. These results suggest that BMP signaling might be a target for the treatment of malignant melanoma. Further studies will be necessary to bridge the gap between the current knowledge on BMP signaling in melanoma and its potential clinical applications.

DATA AVAILABILITY

Data are available on request from the corresponding author.

REFERENCES

1. Tas, F. Metastatic behavior in melanoma: timing, pattern, survival, and influencing factors. *J. Oncol.* **2012**, 647684 (2012).
2. Sandru, A., Voinea, S., Panaitescu, E. & Blidaru, A. Survival rates of patients with metastatic malignant melanoma. *J. Med. Life* **7**, 572–576 (2014).
3. Rapini, R. P., Golitz, L. E., Greer, R. O. Jr, Krekorian, E. A. & Poulson, T. Primary malignant melanoma of the oral cavity. A review of 177 cases. *Cancer* **55**, 1543–1551 (1985).
4. Barker, B. F. et al. Oral mucosal melanomas, the WESTOP Banff workshop proceedings. Western Society of Teachers of Oral Pathology. *Oral Surg. Oral. Med. Oral Pathol. Oral Radiol. Endod.* **83**, 672–679 (1997).
5. Broomhall, C. Malignant melanoma of the oral cavity in Ugandan Africans. *Br. J. Surg.* **54**, 581–584 (1967).
6. Takagi, M., Ishikawa, G. & Mori, W. Primary malignant melanoma of the oral cavity in Japan. With special reference to mucosal melanosis. *Cancer* **34**, 358–370 (1974).
7. Padhye, A. & D'souza, J. Oral malignant melanoma: a silent killer? *J. Indian Soc. Periodontol.* **15**, 425–428 (2011).
8. Ferreira, L., Jham, B., Assi, R., Readinger, A. & Kessler, H. P. Oral melanocytic nevi: a clinicopathologic study of 100 cases. *Oral Surg. Oral Med. Oral Pathol. Oral Radiol.* **120**, 358–367 (2015).
9. Kumar, V. et al. Primary malignant melanoma of oral cavity: a tertiary care center experience. *Natl J. Maxillofac Surg.* **6**, 167–171 (2015).
10. Tchernev, G., Lotti, T. & Wollina, U. Palatal melanoma: "The Silent Killer". *Open Access Maced J. Med. Sci.* **6**, 364–366 (2018).
11. Hsu, M. Y., Rovinsky, S., Penmatcha, S., Herlyn, M. & Muirhead, D. Bone morphogenetic proteins in melanoma: angel or devil? *Cancer Metastasis Rev.* **24**, 251–263 (2005).
12. Jimi, E. The role of BMP signaling and NF-κB signaling on osteoblastic differentiation, cancer development, and vascular diseases-Is the activation of NF-κB a friend or foe of BMP Function? *Vitam. Horm.* **99**, 145–170 (2015).
13. Katagiri, T. & Watabe, T. Bone morphogenetic proteins. *Cold Spring Harb. Perspect. Biol.* **8**, pii: a021899 (2016).
14. Katagiri, T., Tsukamoto, S., Nakachi, Y. & Kuratani, M. Discovery of heterotopic bone-inducing activity in hard tissues and the TGF-β superfamily. *Int. J. Mol. Sci.* **19**, 3586 (2018).
15. De Bosscher, K., Hill, C. S. & Nicolás, F. J. Molecular and functional consequences of Smad4 C-terminal missense mutations in colorectal tumour cells. *Biochem. J.* **379**, 209–216 (2004).
16. Zhou, X. P. et al. Germline mutations in BMPR1A/ALK3 cause a subset of cases of juvenile polyposis syndrome and of Cowden and Bannayan-Riley-Ruvalcaba syndromes. *Am. J. Hum. Genet.* **69**, 704–711 (2001).
17. Jin, Y. et al. Overexpression of BMP-2/4, -5 and BMPR-IA associated with malignancy of oral epithelium. *Oral Oncol.* **37**, 225–233 (2001).
18. Bhowmick, N. A. et al. Transforming growth factor-β1 mediates epithelial to mesenchymal transdifferentiation through a RhoA-dependent mechanism. *Mol. Biol. Cell* **12**, 27–36 (2001).
19. Saika, S. et al. Epithelial–mesenchymal transition as a therapeutic target for prevention of ocular tissue fibrosis. *Endocr. Metab. Immune Disord. Drug Targets* **8**, 69–76 (2008).
20. Voon, D. C., Huang, R. Y., Jackson, R. A. & Thiery, J. P. The EMT spectrum and therapeutic opportunities. *Mol. Oncol.* **11**, 878–891 (2017).
21. Katagiri, T. et al. Identification of a BMP-responsive element in Id1, the gene for inhibition of myogenesis. *Genes Cells* **7**, 949–960 (2002).
22. Akiyama, S. et al. Constitutively active BMP type I receptors transduce BMP-2 signals without the ligand in C2C12 myoblasts. *Exp. Cell Res.* **235**, 362–369 (1997).
23. Furuta, H. et al. Selective inhibition of NF-κB suppresses bone invasion by oral squamous cell carcinoma in vivo. *Int. J. Cancer* **131**, E625–E635 (2012).
24. Tada, Y. et al. The novel IκB kinase β inhibitor IMD-0560 prevents bone invasion by oral squamous cell carcinoma. *Oncotarget* **5**, 12317–12330 (2014).
25. Shin, M. et al. The inhibition of RANKL/RANK signaling by osteoprotegerin suppresses bone invasion by oral squamous cell carcinoma cells. *Carcinogenesis* **32**, 1634–1640 (2011).
26. Rothhammer, T. et al. Bone morphogenic proteins are overexpressed in malignant melanoma and promote cell invasion and migration. *Cancer Res.* **65**, 448–456 (2005).

27. Hsu, M. Y. et al. Aggressive melanoma cells escape from BMP7-mediated autocrine growth inhibition through coordinated Noggin upregulation. *Lab. Invest.* **88**, 842–855 (2008).
28. Braig, S. & Bosserhoff, A. K. Death inducer-obliterator 1 (Dido1) is a BMP target gene and promotes BMP-induced melanomaprogression. *Oncogene* **32**, 837–848 (2013).
29. Park, W. Y., Hong, B. L., Lee, J., Choi, C. & Kim, M. Y. H3K27 Demethylase JMJD3 employs the NF-κB and BMP signaling pathways to modulate the tumor microenvironment and promote melanoma progression and metastasis. *Cancer Res.* **76**, 161–170 (2016).
30. Capasso, M. et al. A predicted functional single-nucleotide polymorphism of bone morphogenetic protein-4 gene affects mRNA expression and shows a significant association with cutaneous melanoma in Southern Italian population. *J. Cancer Res. Clin. Oncol.* **135**, 1799–1807 (2009).
31. Bilodeau, M. L. et al. BMP-2 stimulates tyrosinase gene expression and melanogenesis in differentiated melanocytes. *Pigment Cell Res.* **14**, 328–336 (2001).
32. Tian, H., Zhao, J., Brochmann, E. J., Wang, J. C. & Murray, S. S. Bone morphogenetic protein-2 and tumor growth: diverse effects and possibilities for therapy. *Cytokine Growth Factor Rev.* **34**, 73–91 (2017).
33. Ghosh-Choudhury, N. et al. Bone morphogenetic protein-2 blocks MDA MB 231 human breast cancer cell proliferation by inhibiting cyclin-dependent kinase-mediated retinoblastoma protein phosphorylation. *Biochem. Biophys. Res. Commun.* **272**, 705–711 (2000).
34. Ghosh-Choudhury, N. et al. Bone morphogenetic protein-2 induces cyclin kinase inhibitor p21 and hypophosphorylation of retinoblastoma protein in estradiol-treated MCF-7 human breast cancer cells. *Biochim. Biophys. Acta* **21**, 186–196 (2000).
35. Dumont, N. & Arteaga, C. L. A kinase-inactive type II TGF-β receptor impairs BMP signaling in human breast cancer cells. *Biochem Biophys. Res. Commun.* **301**, 108–112 (2003).
36. Kleeff, J. et al. Bone morphogenetic protein 2 exerts diverse effects on cell growth in vitro and is expressed in human pancreatic cancer in vivo. *Gastroenterology* **116**, 1202–1216 (1999).
37. Langenfeld, E. M. et al. The mature bone morphogenetic protein-2 is aberrantly expressed in non-small cell lung carcinomas and stimulates tumor growth of A549 cells. *Carcinogenesis* **24**, 1445–1454 (2003).
38. Varley, J. E., McPherson, C. E., Zou, H., Niswander, L. & Maxwell, G. D. Expression of a constitutively active type I BMP receptor using a retroviral vector promotes the development of adrenergic cells in neural crest cultures. *Dev. Biol.* **196**, 107–118 (1998).
39. Wang, Y., Zheng, Y., Chen, D. & Chen, Y. Enhanced BMP signaling prevents degeneration and leads to endochondral ossification of Meckel's cartilage in mice. *Dev. Biol.* **381**, 301–311 (2013).
40. Kawamura, C., Kizaki, M. & Ikeda, Y. Bone morphogenetic protein (BMP)-2 induces apoptosis in human myeloma cells. *Leuk. Lymphoma* **43**, 635–639 (2002).
41. Liu, H., Bao, D., Xia, X., Chau, J. F. & Li, B. An unconventional role of BMP-Smad1 signaling in DNA damage response: a mechanism for tumorsuppression. *J. Cell Biochem.* **115**, 450–456 (2014).
42. Venkatesan, A. M. et al. Ligand-activated BMP signaling inhibits cell differentiation and death to promote melanoma. *J. Clin. Investig.* **128**, 294–308 (2018).
43. McCormack, N., Molloy, E. L. & O'Dea, S. Bone morphogenetic proteins enhance an epithelial-mesenchymal transition in normal airway epithelial cells during restitution of a disrupted epithelium. *Respir. Res.* **19**, 14–36 (2013).
44. Davis, H., Raja, E., Miyazono, K., Tsubakihara, Y. & Moustakas, A. Mechanisms of action of bone morphogenetic proteins in cancer. *Cytokine Growth Factor Rev.* **27**, 81–92 (2017).
45. Fang, R. et al. Nodal promotes aggressive phenotype via Snail-mediated epithelial-mesenchymal transition in murine melanoma. *Cancer Lett.* **333**, 66–75 (2013).
46. Hofmann, U. B., Houben, R., Bröcker, E. B. & Becker, J. C. Role of matrix metalloproteinases in melanoma cell invasion. *Biochimie* **87**, 307–314 (2005).
47. Iida, J. & McCarthy, J. B. Expression of collagenase-1 (MMP-1) promotes melanoma growth through the generation of active transforming growth factor-β. *Melanoma Res.* **17**, 205–213 (2007).
48. Rothhammer, T., Braig, S. & Bosserhoff, A. K. Bone morphogenetic proteins induce expression of metalloproteinases in melanoma cells and fibroblasts. *Eur. J Cancer* **44**, 2526–2534 (2008).
49. Huang, Q. et al. IL-1β-induced activation of p38 promotes metastasis in gastric adenocarcinoma via upregulation of AP-1/c-fos, MMP2 and MMP9. *Mol. Cancer* **13**, 18 (2014).
50. Gonzalez, D. M. & Medici, D. Signaling mechanisms of the epithelial-mesenchymal transition. *Sci. Signal.* **7**, re8 (2014).
51. Davis, H., Raja, E., Miyazono, K., Tsubakihara, Y. & Moustakas, A. Mechanisms of action of bone morphogenetic proteins in cancer. *Cytokine Growth Factor Rev.* **27**, 81–92 (2016).

ACKNOWLEDGEMENTS

We thank Dr. Takenobu Katagiri (Saitama Medical University, Saitama, Japan) for providing the d-WT4F-luciferase reporter and the V5-Tagged constitutively active form of BMPRIA (V5-CaALK3/pDEF). This work was supported by a research grant for the OBT Research Center from Kyushu University (to E.J.), and Fukuoka Public Health Promotion Organization Cancer Research Fund (to J.G.)

AUTHOR CONTRIBUTIONS

J.G., R.M., H.F., M.S., M.I., S.C., and E.J. performed the experiments. K.A., Y.T., T.Y., and T. Kukita performed the radiological assessments. K.N., R.M., R.N., T.Y., M.M., and T. Kiyoshima prepared the histological samples. Y.T. and S.F. analyzed TCGA dataset. J.G., T. Kiyoshima, K.O., and Y.M. reviewed the intermediate draft. E.J. designed the study, performed the literature review, prepared the initial, final versions, and revised versions of the paper, and submitted the documents.

COMPETING INTERESTS

The authors declare no competing interests.

ETHICS APPROVAL AND CONSENT TO PARTICIPATE

All experimental procedures conducted in this study were reviewed and approved by the Kyushu University Research Ethics Committee (approval numbers 27–362 and 30–235), and by the Council on Animal Care and Use Committee of Kyushu University (approval number A30-362).

ADDITIONAL INFORMATION

Supplementary information The online version contains supplementary material available at https://doi.org/10.1038/s41374-021-00661-y.

Correspondence and requests for materials should be addressed to Eijiro Jimi.

Reprints and permission information is available at http://www.nature.com/reprints

Publisher's note Springer Nature remains neutral with regard to jurisdictional claims in published maps and institutional affiliations.